Extinction behaviour for two-dimensional inward-solidification problems

By Scott W. McCue, John R. King and David S. Riley

Division of Theoretical Mechanics, School of Mathematical Sciences, University of Nottingham, Nottingham NG7 2RD, UK.

The problem of the inward solidification of a two-dimensional region of fluid is considered, it being assumed that the liquid is initially at its fusion temperature and that heat flows by conduction only. The resulting one-phase Stefan problem is reformulated using the Baiocchi transform and is examined using matched asymptotic expansions under the assumption that the Stefan number is large. Analysis on the first time-scale reveals the liquid-solid free boundary becomes elliptic in shape at times just before complete freezing. However, as with the radially symmetric case considered previously, this analysis leads to an unphysical singularity in the final temperature distribution. A second time-scale therefore needs to be considered, and it is shown the free boundary retains it shape until another non-uniformity is formed. Finally, a third (exponentionally-short) time-scale, which also describes the generic extinction behaviour for all Stefan numbers, is needed to resolve the non-uniformity. By matching between the last two time-scales we are able to determine a uniformly valid description of the temperature field and the location of the free boundary at times just before extinction. Recipes for computing the time it takes to completely freeze the body and the location at which the final freezing occurs are also derived.

Keywords: Stefan problem; extinction behaviour; asymptotic solution

1. Introduction

In this paper we consider the behaviour of inward solidification problems at times just before extinction. Problems of this sort, which involve conduction of heat and a moving interface between different phases, are referred to as Stefan problems. The key parameter in most Stefan problems is the Stefan number, which is defined to be the ratio of latent to sensible heats.

Stefan problems are inherently difficult to treat analytically, as they involve a moving boundary and are hence nonlinear in nature. There is an important exact similarity solution, the Neumann solution (see Carslaw and Jaeger 1973), to the one-dimensional problem, but for more complicated geometries solutions are usually found numerically. There has been recent progress with asymptotic solutions, however, where the Stefan number is considered to be either large or small. For example, Howison and King (1989), Wallman, King and Riley (1997), Hoang, Hill and Dewynne (1998) and King, Riley and Wallman (1999) have studied two-dimensional generalizations of Neumann's one-phase problem in this way.

We are particularly interested here in Stefan problems in which there is a finite region of fluid, initially at fusion temperature, which solidifies inwards due to the

boundary being held at a lower temperature. These problems bring extra difficulties in that the behaviour just before the fluid freezes completely is quite complicated. Numerical studies of inward solidification problems have been undertaken by many authors; for example, see Allen and Severn (1962), Lazaridis (1970), Crank and Gupta (1975), Crowley (1978) and Wallman (1997). Approximate methods have also been used; see Riley and Duck (1976), Davis and Hill (1982), Hill and Dewynne (1986) and the references therein.

For the cases where the fixed boundary is circular or spherical, one can develop perturbation solutions for the (one-phase) inward solidification problem in the limit of large Stefan number (see Pedroso and Domoto 1973 and Riley, Smith and Poots 1974). Under this assumption, the leading order problem becomes quasi-steady, as the solid-liquid interface moves very slowly, and the time derivative of the temperature can be ignored. Such solutions, however, are singular at times close to extinction. Riley, Smith and Poots (1974) use the method of matched asymptotic expansions to deal with this singularity by considering a second time-scale in which it is no longer appropriate to neglect the time derivative. It happens that this solution also becomes singular, and further analysis in a third, exponentially short time-scale has been undertaken by both Stewartson and Waechter (1976) (spherical boundary) and Soward (1980) (both circular and spherical boundaries) to complete the asymptotic description.

The analysis on the third and final time-scale presented by Soward (1980) is actually valid for all values of the Stefan number (though for the special case of large Stefan number, the matching between second and third time-scales fixes asymptotically the value of a free constant); cf. Herrero and Velázquez (1997). Andreucci, Herrero and Velázquez (2001), in work that appeared after the current analysis was essentially completed, have extended this generic extinction analysis to truely two- and three-dimensional geometries. They show that, regardless of the Stefan number, the shrinking region of liquid is elliptic in shape in two dimensions, and ellipsoidal in three dimensions, just before complete freezing takes place. They also derive the time-dependence of the behaviour as the region of liquid vanishes.

The present study was motivated in part by numerical results of Wallman (1997) for the solidification of a rectangle. These indicated that the aspect ratio of the liquid domain increases significantly as freezing proceeds and, moreover, that the moving boundary can be represented very accurately by an ellipse for times sufficiently close to complete solidification. Rather close to the extinction time, the eccentricity of this ellipse was seen to level off to a value dependent on the Stefan number and the aspect ratio of the domain. However, extremely close to extinction the ellipse evolved very rapidly to a circle; despite careful remeshing about the extinction point it was unclear whether this final stage was a numerical artefact; the current analysis shows that this in fact is the case (see also Andreucci *et al.* 2001). In the present study, we extend the analysis of Soward (1980) by considering the near extinction behaviour when a general two-dimensional region of fluid is solidified at large Stefan number. The leading order equations in the first time-scale are equivalent to those governing the contraction of a bubble in a Hele-Shaw cell, and have been studied by Entov and Etingof (1991) and McCue, King and Riley (2003). Entov and Etingof compute the location of the extinction point within the initial domain as well as the time it takes for the bubble to vanish. They also show the shape of the shrinking bubble is generically elliptic, regardless of the initial domain.

In an appendix, McCue *et al.* give a recipe for computing the aspect ratio of the shrinking bubble, and compute the rates at which these elliptic bubbles vanish.

As with the earlier radial analyses, a non-uniformity appears on the first time-scale, and hence further analysis on a second time-scale is needed. We show that the elliptic shape of the solid-melt interface continues through the second time-scale, maintaining the aspect ratio attained over the first time-scale. We also derive a recipe for computing a number of correction terms in a large Stefan number approximation of the extinction time, these being dependent only on the shape of the domain. This analysis in turn breaks down at times exponentially close to extinction, resulting in a logarithmic singularity in the final temperature distribution. To complete the analysis we need to match with the resulting (third) time-scale, which is described by the generic extinction analysis also examined in Andreucci *et. al* (2001).

In section 2 we formulate the solidification problem for a general two-dimensional geometry, and introduce the Baiocchi transform, which we use throughout the paper. Section 3 summarises the generic extinction behaviour for arbitrary Stefan number, while section 4 presents the new analysis for large Stefan number. As a simple example, we show in section 5 how some of the results can be applied to the case in which the domain is rectangular. Comparisons are also made with the numerical results obtained by Wallman (1997). Finally, the paper is closed in section 6 with discussion.

2. Mathematical formulation

Consider a simply connected region of fluid B^* which is initially at its fusion temperature $u^* = u_F^*$ and with the fixed boundary ∂B^* held at a lower temperature $u^* = u_W^*$. As a result of this change in temperature, the fluid will solidify inwards.

If we assume that the heat flows through conduction only, that the thermal diffusivity κ and the specific heat (at constant pressure) c_p of the solid are constant and that the density is the same constant in both phases, then the problem is to solve the heat equation

$$\frac{\partial u^*}{\partial t^*} = \kappa \left(\frac{\partial^2 u^*}{\partial x^{*2}} + \frac{\partial^2 u^*}{\partial y^{*2}} \right)$$

in the solid region, with the condition $u^* = u_W^*$ on the fixed boundary ∂B^*, and also

$$u^* = u_F^*, \quad \frac{L}{\kappa c_p} = \boldsymbol{\nabla}^* u^* \cdot \boldsymbol{\nabla}^* \omega^*$$

on the moving interface, which we denote by $t^* = \omega^*(x^*, y^*)$. Here L is the latent heat of fusion per unit mass.

We scale all quantities by introducing the dimensionless variables

$$t = \frac{\kappa t^*}{l^{*2}}, \quad x = \frac{x^*}{l^*}, \quad y = \frac{y^*}{l^*}, \quad u = \frac{u^* - u_F^*}{u_F^* - u_W^*}, \quad \omega = \frac{\kappa \omega^*}{l^{*2}},$$

where l^* is some representative length-scale of B^*. It follows that our problem reduces to solving

$$\frac{\partial u}{\partial t} = \frac{\partial^2 u}{\partial x^2} + \frac{\partial^2 u}{\partial y^2} \tag{2.1}$$

throughout the solid region, subject to the boundary conditions

$$u = -1 \quad \text{on} \quad \partial B; \quad u = 0, \quad \beta = \boldsymbol{\nabla} u \cdot \boldsymbol{\nabla} \omega \quad \text{on} \quad t = \omega(x, y), \tag{2.2}$$

where the one parameter in the problem (other than those pertaining to the geometry ∂B) is the Stefan number, defined by

$$\beta = \frac{L}{c_p(u_F^* - u_W^*)}.$$

Note that the intial region of fluid in non-dimensional coordinates is denoted by B and its boundary by ∂B.

It will prove very useful to work with the Baiocchi transform, defined by

$$w(x, y, t) = -\int_{\omega(x,y)}^{t} u(x, y, t')\, dt'. \tag{2.3}$$

In terms of w, the governing equation is

$$\frac{\partial w}{\partial t} = \frac{\partial^2 w}{\partial x^2} + \frac{\partial^2 w}{\partial y^2} - \beta, \tag{2.4}$$

and the boundary conditions become

$$w = \frac{\partial w}{\partial n} = 0 \quad \text{on} \quad t = \omega(x, y), \tag{2.5}$$

$$w = t \quad \text{on} \quad \partial B. \tag{2.6}$$

Given a solution w, the temperature u can be recovered via $u = -\partial w/\partial t$, or via $u = -\nabla^2 w + \beta$.

We will denote the time it takes to complete freezing (the extinction time) by t_f, so that the problem is to describe the temperature field and the location of the free boundary as $t \to t_f^-$. We shall also use another temporal variable τ, defined by $\tau = t_f - t$, as well as the new function Ω, defined by $\Omega(x, y) = t_f - \omega(x, y)$, so the free boundary is given by $\tau = \Omega(x, y)$.

3. Generic extinction behaviour

(a) *Preamble*

Here we describe the asymptotic solution to (2.4)-(2.6) in the limit $t \to t_f^-$ (or, equivalently, in the limit $\tau \to 0^+$), for arbitrary Stefan number β. For this analysis we locate the extinction point at the origin.

The results given here are important for large Stefan number asymptotics, since the final exponentially short time-scale is described here. The analysis presented in this section is needed to determine the matching with the second time-scale described later, which in turn completes the determination of the relationship between the aspect ratio of the evolving free boundary just before extinction and both the Stefan number β and the initial geometry B. We also require this analysis to determine final temperature distribution near the extinction point and the rate at

which the free boundary contracts, the former becoming singular on the second time-scale. With these quantities determined, it becomes clear when and where the description for the second time-scale becomes invalid. Results equivalent to those of this section have been derived by Andreucci *et al.* (2001); we believe our approach to be more transparent, though lacking in rigour.

To discuss the limit $x, y, \tau \to 0$, we introduce the similarity variables

$$\xi = \frac{x}{\tau^{1/2}}, \quad \eta = \frac{y}{\tau^{1/2}}, \quad \rho = \frac{r}{\tau^{1/2}}, \quad T = -\log\tau, \tag{3.1}$$

$$w(x, y, \tau) = \tau\beta W(\xi, \eta, T), \quad \Lambda(\xi, \eta) = -\log(\Omega(x, y)),$$

so that equations (2.4) and (2.5) become

$$\frac{\partial^2 W}{\partial\xi^2} + \frac{\partial^2 W}{\partial\eta^2} - \frac{1}{2}\xi\frac{\partial W}{\partial\xi} - \frac{1}{2}\eta\frac{\partial W}{\partial\eta} + W = \frac{\partial W}{\partial T} + 1, \tag{3.2}$$

$$W = \frac{\partial W}{\partial\nu} = 0 \quad \text{on} \quad T = \Lambda(\xi, \eta), \tag{3.3}$$

where $\partial/\partial\nu$ denotes the derivative in the normal direction.

(*b*) *Inner region,* $\xi, \eta = O(\sigma)$

We define σ such that the area enclosed by the free boundary is $\pi\tau\sigma(T)^2$ and introduce the variables $\hat{\xi} = \xi/\sigma$, $\hat{\eta} = \eta/\sigma$, with $\sigma \ll 1$ to be determined. In this region $\xi^2 + \eta^2 = O(\sigma^2)$ and

$$W \sim \sigma(T)^2\Phi_0(\hat{\xi}, \hat{\eta}) + O(\sigma^4) \quad \text{as} \quad T \to \infty, \tag{3.4}$$

where the dot denotes a derivative with respect to T, so that to leading order (3.2)-(3.3) give

$$\frac{\partial^2\Phi_0}{\partial\hat{\xi}^2} + \frac{\partial^2\Phi_0}{\partial\hat{\eta}^2} = 1, \quad \Phi_0 = \frac{\partial\Phi_0}{\partial\hat{\nu}} = 0 \quad \text{on the free boundary.} \tag{3.5}$$

In order to match with the intermediate region described below, the far-field condition must be of the form

$$\Phi_0 = a_1(\hat{\xi}\cos\hat{\theta} + \hat{\eta}\sin\hat{\theta})^2 + (\tfrac{1}{2} - a_1)(-\hat{\xi}\sin\hat{\theta} + \hat{\eta}\cos\hat{\theta})^2 - \tfrac{1}{4}\log(\hat{\xi}^2 + \hat{\eta}^2) + O(1) \tag{3.6}$$

as $\hat{\xi}^2 + \hat{\eta}^2 \to \infty$, where the constant in front of the logarithm is dictated by our definition of σ. Here a_1 is a free constant ($0 < a_1 < \frac{1}{4}$), which we shall later determine for $\beta \gg 1$ by matching back onto earlier time-scales. The constant $\hat{\theta}$ can also be determined in a similar way when $\beta \gg 1$, but in any case is only a measure of rotation about the origin; without any loss of generality we rotate axes by $\hat{\theta}$ to set $\hat{\theta} = 0$.

The solution to (3.5)-(3.6) is $\Phi_0 = \Psi(\hat{\phi}, \hat{\psi}; a_1)$, where $\Psi(\tilde{\phi}, \tilde{\psi}; \tilde{a})$ is given by

$$\Psi = P_1(\tilde{\phi}) + P_2(\tilde{\phi})\cos 2\tilde{\psi}, \tag{3.7}$$

$$P_1 = \frac{1 - 4\tilde{a}}{16\tilde{a}(1 - 2\tilde{a})}(4\tilde{a} - 1 + \cosh 2\tilde{\phi}) - \tfrac{1}{2}\tilde{\phi} - \tfrac{1}{4}\log(1 - 4\tilde{a}) - \tfrac{1}{4}, \tag{3.8}$$

$$P_2 = \frac{1-4\tilde{a}}{16\tilde{a}(1-2\tilde{a})}(1+(4\tilde{a}-1)\cosh 2\tilde{\phi}) - \tfrac{1}{4}e^{-2\tilde{\phi}}, \tag{3.9}$$

and $(\hat{\phi},\hat{\psi})$ are elliptic coordinates defined by

$$\hat{\xi}+i\hat{\eta} = \left(\frac{1-4a_1}{2a_1(1-2a_1)}\right)^{1/2}\cosh(\hat{\phi}+i\hat{\psi}).$$

The free boundary is elliptic in shape, with aspect ratio $(1-2a_1)/2a_1$ and eccentricity $(1-4a_1)^{1/2}/(1-2a_1)$. It is the curve upon which $\hat{\phi} = -\frac{1}{2}\log(1-4a_1)$; equivalently, it is given the original variables by

$$\frac{2a_1}{1-2a_1}\,x^2 + \frac{1-2a_1}{2a_1}\,y^2 = \tau\sigma^2. \tag{3.10}$$

To match with the intermediate region we need the far-field behaviour (including $O(1)$ terms), whereby

$$\Phi_0 \sim a_1\hat{\xi}^2 + (\tfrac{1}{2}-a_1)\hat{\eta}^2 - \tfrac{1}{4}\log(\hat{\xi}^2+\hat{\eta}^2) - \tfrac{1}{4}(1+\log(8a_1(1-2a_1))) \tag{3.11}$$

as $\hat{\xi},\hat{\eta}\to\infty$.

(*c*) *Intermediate region,* $\xi^2+\eta^2 = O(1)$

Here we use polar coordinates (ρ,θ) and expand

$$W \sim a_1\xi^2 + (\tfrac{1}{2}-a_1)\eta^2 + B(T)W_1(\rho,\theta) + \dot{B}(T)W_2(\rho,\theta) + \ddot{B}(T)W_3(\rho,\theta) \tag{3.12}$$

as $T\to\infty$. In order to match with (3.11) we require that the W_i behave as

$$W_i \sim k_{i1}\log\rho + k_{i2} \quad \text{as} \quad \xi,\eta\to 0 \tag{3.13}$$

for $i=1,2,3,4$, where the k_{i1} are constants found as part of the solution process (the far-field behaviour of the higher-order terms in (3.4) is consistent with (3.13)). We specify the as yet unknown function $B(T)$ uniquely by imposing the conditions

$$k_{12}=1, \quad k_{i2}=0, \quad i\geq 2. \tag{3.14}$$

It is assumed that $|\ddot{B}(T)| \ll |\dot{B}(T)| \ll |B(T)|$ as $T\to\infty$ (conditions which can be verified *posterior*), so that substituting (3.12) into (3.2) provides

$$\frac{\partial^2 W_i}{\partial\rho^2} + \left(\frac{1}{\rho}-\frac{1}{2}\rho\right)\frac{\partial W_i}{\partial\rho} + \frac{1}{\rho^2}\frac{\partial^2 W_i}{\partial\theta^2} + W_i = W_{i-1}, \tag{3.15}$$

for $i=1,2,3,4$, with W_0 set to zero.

It is shown in the Appendix that the only solutions to (3.15) which satisfy the conditions (3.13) and (3.14) and do not grow exponentially as $\rho\to\infty$ are those for which the W_i are independent of θ; these are

$$W_1 = -\tfrac{1}{4}\rho^2+1, \quad W_2 = \tfrac{1}{2}\rho^2\log\rho - \tfrac{1}{2}\rho^2 - 2\log\rho, \tag{3.16}$$

$$W_3 = -\tfrac{1}{2}\rho^2\log^2\rho + \rho^2\log\rho - \tfrac{1}{8}(\tfrac{1}{2}\pi^2 + (1+\gamma-2\log 2)^2+7)\rho^2 + 2\log^2\rho$$

$$+E_1(\tfrac{1}{4}\rho^2)e^{\rho^2/4} - \tfrac{1}{2}(4-\rho^2)\int_\rho^\infty \frac{E_1(\frac{1}{4}s^2)e^{s^2/4}}{s}\,ds + \tfrac{1}{2}(\tfrac{1}{2}\pi^2 + (1+\gamma-2\log 2)^2 - 1),$$

$$k_{11} = 0, \quad k_{21} = -2, \quad k_{31} = -2(1+\gamma-2\log 2),$$

where $E_1(z)$ is the Exponential Integral defined by

$$E_1(z) = \int_z^\infty \frac{e^{-s}}{s}\,ds\,, \quad \text{for} \quad z > 0. \tag{3.17}$$

Further calculations reveal that

$$k_{41} = -1 + \tfrac{1}{6}\pi^2 - (1+\gamma-2\log 2)^2$$

so the matching with (3.11) thus implies that

$$\dot{B} + (1+\gamma-2\log 2)\ddot{B} + \tfrac{1}{2}(1 - \tfrac{1}{6}\pi^2 + (1+\gamma-2\log 2)^2)\dddot{B} \sim \tfrac{1}{4}\sigma^2 \tag{3.18}$$

$$B \sim \tfrac{1}{2}\sigma^2\log\sigma - \tfrac{1}{4}\sigma^2(1+\log(8a_1(1-2a_1))).$$

These two equations can be solved asymptotically to give

$$B = -8a_1\sqrt{2}(1-2a_1)(T+T_c)^{1/2}e^{-(1+\gamma)}e^{-\sqrt{2}(T+T_c)^{1/2}}\left[1 + \frac{(1-\frac{1}{6}\pi^2)\log(T+T_c)+O(1)}{2\sqrt{2}(T+T_c)^{1/2}}\right] \tag{3.19}$$

$$\sigma = 4(2a_1(1-2a_1))^{1/2}e^{-(1+\gamma)/2}e^{-(T+T_c)^{1/2}/\sqrt{2}}\left[1 + \frac{(1-\frac{1}{6}\pi^2)\log(T+T_c)+O(1)}{4\sqrt{2}(T+T_c)^{1/2}}\right] \tag{3.20}$$

as $T \to \infty$, where T_c is a free constant which depends on the evolution over earlier times. We keep T_c here because for large Stefan number we find $T_c \gg 1$ and the above results are then valid for $T = O(T_c) \gg 1$; we note that T_c corresponds to a shift in T and hence via (3.1) to a rescaling in the spatial and temporal variables. We also note that the correction terms in (3.4) contribute only $O(\sigma^4)$ terms in (3.18), and hence are negligible when matching with the intermediate region.

In order to derive matching conditions for the outer region we first note that

$$W_3 \sim -\tfrac{1}{2}\rho^2\log^2\rho + \rho^2\log\rho - \tfrac{1}{2}(2-\log 2)\rho^2 + 2\log^2\rho + 1 - 2\log 2 \tag{3.21}$$

as $\rho \to \infty$. For convenience the variable

$$R = -\log r = \tfrac{1}{2}T - \log\rho$$

is now introduced, and it is noted that $R = \frac{1}{2}T + O(1)$ in the intermediate region. Taylor expansions for $B(T)$ and its derivatives can now be used (along with (3.16), (3.21)) to give

$$W \sim a_1\xi^2 + (\tfrac{1}{2}-a_1)\eta^2 - \tfrac{1}{4}\rho^2[B(2R) + 2\dot{B}(2R) + 2(2-\log 2)\ddot{B}(2R) + \ldots]$$

$$+[B(2R) + (1-2\log 2)\ddot{B}(2R) + \ldots] + O(\rho^{-2}) \quad \text{as} \quad \rho \to \infty, \tag{3.22}$$

where here the ellipses denote terms of order $\dddot{B}(2R)$ as $R \to \infty$.

(d) *Outer region,* $x^2 + y^2 = O(1)$

In the outer region

$$w \sim w_f(x,y) + \tau u_f(x,y) + O(\tau^2) \quad \text{as} \quad \tau \to 0,$$

with

$$\nabla^2 w_f = -u_f + \beta \quad \text{in} \quad B, \quad w_f = t_f, \quad u_f = -1 \quad \text{on} \quad \partial B, \tag{3.23}$$

where $w_f = w(x,y,t_f)$ and $u_f = u(x,y,t_f)$. Here u_f is determined by evolution over earlier times, and w_f is given in terms of u_f by the linear boundary-value problem (3.23). In order to match with(3.22) we require that

$$w_f \sim \beta(a_1 x^2 + (\tfrac{1}{2} - a_1)y^2) - \tfrac{1}{4}\beta r^2[B(2R) + 2\dot{B}(2R) + 2(2 - \log 2)\ddot{B}(2R) + \ldots]$$

$$u_f \sim \beta[B(2R) + (1 - 2\log 2)\ddot{B}(2R) + \ldots]$$

as $r \to 0$. That is, for small r we have the following results for extinction time behaviour

$$w_f = \beta(a_1 x^2 + (\tfrac{1}{2} - a_1)y^2) + 4\beta a_1(1-2a_1)e^{-(1+\gamma)}r^2(-\log r + \tfrac{1}{2}T_c)^{1/2}e^{-2(-\log r + T_c/2)^{1/2}}$$
$$\times \left[1 + \frac{(1 - \frac{1}{6}\pi^2)\log(-\log r + T_c/2) + O(1)}{4(-\log r + T_c/2)^{1/2}}\right] \tag{3.24}$$

$$u_f = -16a_1(1-2a_1)\beta e^{-(1+\gamma)}(-\log r + \tfrac{1}{2}T_c)^{1/2}e^{-2(-\log r + T_c/2)^{1/2}}$$
$$\times \left[1 + \frac{(1 - \frac{1}{6}\pi^2)\log(-\log r + T_c/2) + O(1)}{4(-\log r + T_c/2)^{1/2}}\right], \tag{3.25}$$

which are valid providing $r \ll e^{-T_c/2}$ (remembering that we find T_c to be large for $\beta \gg 1$) and approach zero more slowly than algebraically in r. While the solid-melt interface is elliptic just before extinction, the final temperature distribution in the neighbourhood of the extinction point is thus radially symmetric.

(e) *Special case,* $a_1 = \frac{1}{4}$

When $a_1 = \frac{1}{4}$ the local behaviour near the extinction point is radially symmetric, and the circular free boundary can be described by $\rho = \sigma(T)$. The asymptotic expressions for σ and u_f in (3.20) and (3.25) agree with the corresponding results of Soward (1980), who considered the radially symmetric problem. We should note that $a_1 = \frac{1}{4}$ holds for any geometry B which has two axes of reflectional symmetry, for example, as well as for circular domains.

4. Large Stefan number asymptotics

(a) *Preamble*

In the previous section we considered the extinction behaviour of the two-dimensional Stefan problem (2.4)-(2.6). Matched asymptotics were used to derive results for the shape of the free boundary, as well as for the temperature field in the vicinity of the extinction point, in the limit $t \to t_f^-$. Of course, both the extinction

time and the location of the extinction point depend on the domain B and the Stefan number β, as do the values of the constants T_c and a_1. However, in general, the nonlinearity of the equations (2.4)-(2.6) does not allow one to determine these quantities analytically. An important exception, however, is the physically important limit of large Stefan number, $\beta \gg 1$. In this case it is possible to use large β asymptotics to treat the problem on earlier time-scales, allowing the formulation of recipes for computing the extinction time t_f and the location of the extinction point. In addition, the matching between results in section 3 and these earlier time-scales allows the determination of the constants T_c and a_1. We now present the analysis for $\beta \gg 1$, noting it is an extension of that presented by Riley, Smith and Poots (1974) and Soward (1980) to general two-dimensional domains.

(*b*) *Time-scale 1,* $t = O(\beta)$

(i) *Leading-order formulation*

On the first time-scale the solid-melt interface moves very slowly because of the need to remove the large amounts of latent heat produced. We introduce the temporal variable $\hat{t} = t/\beta$, and write

$$w \sim \beta w_0(x, y, \hat{t}), \quad \omega \sim \beta \hat{\omega}_0(x, y) \quad \text{as} \quad \beta \to \infty,$$

so that the leading order problem reads

$$\frac{\partial^2 w_0}{\partial x^2} + \frac{\partial^2 w_0}{\partial y^2} = 1, \tag{4.1}$$

with

$$w_0 = \hat{t} \quad \text{on} \quad \partial B, \quad w_0 = \frac{\partial w_0}{\partial n} = 0 \quad \text{on} \quad \hat{t} = \hat{\omega}_0(x, y). \tag{4.2}$$

The temporal derivative is thus negligible, the leading order equations depending on $\hat{t}$ only parametrically. These equations describe an extinction problem in their own right, and in fact govern the contraction of a bubble of air in an otherwise filled Hele-Shaw cell (see Entov and Etingof 1991, for example).

We let the extinction time for this leading-order problem be $\hat{t}_e$, denote the point at which extinction occurs by (x_e, y_e) and set $w_e(x, y) = w_0(x, y, \hat{t}_e)$. Although it is not in general possible to solve the nonlinear problem (4.1)-(4.2) for all time $\hat{t}$, we can extract all required information by taking advantage of the quasi-steadiness of the equations and considering the solution at times leading up to extinction. The following analysis of the leading order solution summaries that in McCue *et al.* (2003).

We can compute w_e by setting $w_e = W_e(x, y) + \hat{t}_e$ and solving the linear boundary-value problem

$$\frac{\partial^2 W_e}{\partial x^2} + \frac{\partial^2 W_e}{\partial y^2} = 1 \quad \text{in} \quad B \quad \text{with} \quad W_e = 0 \quad \text{on} \quad \partial B. \tag{4.3}$$

The point (x_e, y_e) is where W_e achieves a global minimum (for simplicity we assume there to be only one such point) and the extinction time $\hat{t}_e$ is found from $\hat{t}_e = -W_e(x_e, y_e)$. The function w_e has the behaviour

$$w_e(x, y) \sim a\tilde{x}^2 + \left(\tfrac{1}{2} - a\right)\tilde{y}^2 \quad \text{as} \quad (x, y) \to (x_e, y_e), \tag{4.4}$$

where the Cartesian coordinates $(\tilde{x}, \tilde{y})$, defined by

$$\tilde{x} = (x - x_e)\cos\tilde{\theta} + (y - y_e)\sin\tilde{\theta}, \quad \tilde{y} = -(x - x_e)\sin\tilde{\theta} + (y - y_e)\cos\tilde{\theta},$$

are formed by a translation and rotation from (x, y). The constant a, which lies in the range $0 \leq a \leq \frac{1}{4}$, can be determined exactly only if (4.3) can be solved explicitly (see section 5 for an example), otherwise one would have to resort to numerical methods; similar comments apply to (x_e, y_e) and $\tilde{\theta}$, though symmetries of the domain may enable their values to be identified *a priori*. Without any loss of generality we shall assume that $\tilde{\theta} = x_e = y_e = 0$, so that the point of extinction coincides with the origin and in the limit $\hat{t} \to \hat{t}_e^-$ the local behaviour (4.4) of the function w_e is symmetric about both the x and the y axes. The expression (4.4) then takes the form

$$w_e \sim ax^2 + (\tfrac{1}{2} - a)y^2 \quad \text{as} \quad x, y \to 0. \tag{4.5}$$

(ii) *Inner region, $x, y = O(\bar{T})$*

As $\hat{t} \to \hat{t}_e^-$, there are two spatial regions to consider. The inner region corresponds to $r = O(\bar{T})$, where the function $\bar{T}(\hat{t}_e - \hat{t})$, which remains to be determined but satisfies $\bar{T} \to 0$ as $\hat{t} \to \hat{t}_e^-$, is defined so that the area enclosed by the free boundary $\hat{t} = \hat{\omega}_0$ is $\pi\bar{T}^2$. We introduce the variables $X = x/\bar{T}$, $Y = y/\bar{T}$, $R = r/\bar{T}$ and denote the region inside the free boundary in (X, Y) space by Γ_0. By writing

$$w_0 \sim \bar{T}^2\Phi(X, Y) \quad \text{as} \quad \bar{T} \to 0, \tag{4.6}$$

we arrive at the boundary-value problem for Φ:

$$\frac{\partial^2\Phi}{\partial X^2} + \frac{\partial^2\Phi}{\partial Y^2} = 1 \quad \text{outside} \quad \Gamma_0, \tag{4.7}$$

$$\Phi = \frac{\partial\Phi}{\partial N} = 0 \quad \text{on} \quad \partial\Gamma_0, \tag{4.8}$$

$$\Phi \sim aX^2 + \left(\tfrac{1}{2} - a\right)Y^2 - \tfrac{1}{4}\log(X^2 + Y^2) + O(1) \quad \text{as} \quad X^2 + Y^2 \to \infty, \tag{4.9}$$

where $\partial/\partial N$ is used to denote the rescaled normal derivative and $\partial\Gamma_0$ the boundary of Γ_0. The quadratic terms in (4.9) are included in anticipation of a match with (4.5), while the coefficient in front of the logarithm follows because the area of Γ_0 is required by our definition of $\bar{T}$ to be π.

The solution to (4.7)-(4.9) is given by $\Phi = \Psi(\phi, \psi; a)$, where the function Ψ is defined in (3.7)-(3.9) and (ϕ, ψ) are elliptic coordinates defined by

$$X + iY = \left(\frac{1 - 4a}{2a(1 - 2a)}\right)^{1/2} \cosh(\phi + i\psi). \tag{4.10}$$

The boundary $\partial\Gamma_0$ is the ellipse

$$\left(\frac{2a}{1 - 2a}\right)X^2 + \left(\frac{1 - 2a}{2a}\right)Y^2 = 1, \tag{4.11}$$

which has an aspect ratio $(1 - 2a)/2a$ and eccentricity $(1 - 4a)^{1/2}/(1 - 2a)$.

To match with the outer region, we set $X = x/\bar{T}$, $Y = y/\bar{T}$ in (4.6) and expand in $\bar{T}$. This process yields as a matching condition on the outer region that

$$w_0 \sim ax^2 + \left(\tfrac{1}{2} - a\right) y^2 - \tfrac{1}{4}\bar{T}^2\{\log(x^2+y^2) - 2\log\bar{T} + 1 + \log(8a(1-2a))\} + O(\bar{T}^4), \tag{4.12}$$

as $x, y, \bar{T} \to 0$.

(iii) *Outer region, $x^2 + y^2 = O(1)$*

The outer region corresponds to $r = O(1)$. Here the appropriate expansion for w_0 takes the form

$$w_0 \sim w_e(x,y) - (\hat{t}_e - \hat{t}) + \mu(\bar{T})\Lambda(x,y) \quad \text{as} \quad \hat{t} \to \hat{t}_e^-, \tag{4.13}$$

where μ vanishes faster than linearly as $\hat{t} \to \hat{t}_e^-$, and Λ is harmonic and vanishes on ∂B. To match with (4.12) we must choose $\mu = \bar{T}^2$, so that $\Lambda \sim -\frac{1}{4}\log(x^2+y^2)$ as $x, y \to 0$. It follows that $\Lambda = \pi G$, where G is the Green's function which satisfies

$$-\left(\frac{\partial^2 G}{\partial x^2} + \frac{\partial^2 G}{\partial y^2}\right) = \delta(x)\delta(y) \quad \text{in} \quad B \quad \text{with} \quad G = 0 \quad \text{on} \quad \partial B, \tag{4.14}$$

and has the local behaviour

$$G \sim -\frac{1}{2\pi}(\log r + K) \quad \text{as} \quad r \to 0 \tag{4.15}$$

for some constant K which depends on B. To complete the matching with (4.12) we require that

$$\hat{t}_e - \hat{t} \sim -\tfrac{1}{2}\bar{T}^2\log\bar{T} + \tfrac{1}{4}\bar{T}^2\{1 + \log(8a(1-2a)) - 2K\} + O(\bar{T}^4) \quad \text{as} \quad \bar{T} \to 0,$$

so

$$\bar{T} \sim \frac{2(\hat{t}_e - \hat{t})^{1/2}}{\log^{1/2}(1/(\hat{t}_e - \hat{t}))}\left[1 - \frac{\log\log(1/(\hat{t}_e - \hat{t})) + 1 + \log[2a(1-2a)] - 2K}{2\log(1/(\hat{t}_e - \hat{t}))}\right] \tag{4.16}$$

as $\hat{t} \to \hat{t}_e^-$.

(*c*) *Time-scale 2, $t_f - t = O(1)$*

(i) *Introduction*

The second time-scale is for $\tau = t_f - t = O(1)$. The solid-melt interface is rapidly moving, and at order one distances away from the extinction point the leading order temperature evolution is no longer quasi-steady. It follows from (4.16) that the area enclosed by the free boundary on this second time-scale is $O(\epsilon^2)$, where $\epsilon \ll 1$ is defined by

$$\frac{1}{\beta} = \epsilon^2\log(1/\epsilon). \tag{4.17}$$

The expansion for the extinction time t_f then takes the form

$$t_f = \beta\tau_a + \tau_b + \frac{\tau_c}{\log(1/\epsilon)} + \frac{\tau_d}{\log^2(1/\epsilon)} + O(\log^{-3}(1/\epsilon)), \tag{4.18}$$

where the τ_j, $j = a, b, c, d$ are to be determined.

(ii) *Region I (inner), $x, y = O(\epsilon)$*

There are two spatial regions to consider over the second time-scale. In the first region we use the scaled variables

$$\bar{x} = \frac{x}{\epsilon}, \quad \bar{y} = \frac{y}{\epsilon}, \quad \bar{r} = \frac{r}{\epsilon},$$

and write

$$w = \frac{1}{\log(1/\epsilon)}\,\bar{W}_1(\bar{x},\bar{y},\tau) + \frac{1}{\log^2(1/\epsilon)}\,\bar{W}_2(\bar{x},\bar{y},\tau) + O(\log^{-3}(1/\epsilon)),$$

where ϵ is defined by (4.17). By expanding the free boundary description as

$$\Omega = \Omega_0(\bar{x},\bar{y}) + \frac{1}{\log(1/\epsilon)}\,\Omega_1(\bar{x},\bar{y}) + O(\log^{-2}(1/\epsilon)),$$

we can derive the governing equations for $\bar{W}_1$ and $\bar{W}_2$ in the form

$$\frac{\partial^2 \bar{W}_1}{\partial \bar{x}^2} + \frac{\partial^2 \bar{W}_1}{\partial \bar{y}^2} = 1 \quad \text{outside} \quad \tau = \Omega_0(\bar{x},\bar{y}), \tag{4.19}$$

$$\bar{W}_1 = \frac{\partial \bar{W}_1}{\partial \bar{n}} = 0 \quad \text{on} \quad \tau = \Omega_0(\bar{x},\bar{y}) \tag{4.20}$$

$$\bar{W}_1 \sim \bar{a}\bar{x}^2 + \left(\tfrac{1}{2} - \bar{a}\right)\bar{y}^2 + \tfrac{1}{2} f_1(\tau)\log(\bar{x}^2+\bar{y}^2) + h_1(\tau) \quad \text{as} \quad \bar{x}^2+\bar{y}^2 \to \infty \tag{4.21}$$

and

$$\frac{\partial^2 \bar{W}_2}{\partial \bar{x}^2} + \frac{\partial^2 \bar{W}_2}{\partial \bar{y}^2} = 0 \quad \text{outside} \quad \tau = \Omega_0(\bar{x},\bar{y}), \tag{4.22}$$

$$\bar{W}_2 = 0, \quad \Omega_1 \frac{\partial^2 \bar{W}_1}{\partial \tau \partial \bar{n}} + \frac{\partial \bar{W}_2}{\partial \bar{n}} = 0 \quad \text{on} \quad \tau = \Omega_0(\bar{x},\bar{y}), \tag{4.23}$$

$$\bar{W}_2 \sim \tfrac{1}{2} f_2(\tau)\log(\bar{x}^2+\bar{y}^2) + h_2(\tau) \quad \text{as} \quad \bar{x}^2+\bar{y}^2 \to \infty, \tag{4.24}$$

where $\partial/\partial\bar{n}$ denotes the normal derivative. Here $\bar{a}$ is constant, which can easily be seen to be given by $\bar{a} = a$ by matching back into the first time-scale. The functions $f_i(\tau)$ and $h_i(\tau)$ are as yet unknown, and will be determined through matching with region II in the present time-scale. We solve (4.19)-(4.21) and (4.22)-(4.24) later; see section 4c(iv).

(iii) *Region II (outer), $x^2 + y^2 = O(1)$*

For this second spatial region on the second time-scale, we write

$$w \sim \beta w_a(x,y) - \tau + w_b(x,y) + \frac{1}{\log(1/\epsilon)}\,\tilde{W}_1(x,y,\tau) + \frac{1}{\log^2(1/\epsilon)}\,\tilde{W}_2(x,y,\tau) \tag{4.25}$$

By substituting (4.25) in (2.4)-(2.6) we find that

$$\frac{\partial^2 w_j}{\partial x^2} + \frac{\partial^2 w_j}{\partial y^2} = 1 \quad \text{in} \quad B, \quad w_j = \tau_j \quad \text{on} \quad \partial B, \tag{4.26}$$

$$w_j = \frac{\partial w_j}{\partial x} = \frac{\partial w_j}{\partial y} = 0 \quad \text{at} \quad (x,y) = (0,0), \tag{4.27}$$

for $j = a, b$, and

$$\frac{\partial^2 \tilde{W}_i}{\partial x^2} + \frac{\partial^2 \tilde{W}_i}{\partial y^2} = -\frac{\partial \tilde{W}_i}{\partial \tau} \quad \text{in} \quad B \tag{4.28}$$

$$\tilde{W}_1 = \tau_c, \quad \tilde{W}_2 = \tau_d \quad \text{on} \quad \partial B, \tag{4.29}$$

$$\tilde{W}_i \sim \tfrac{1}{2} F_i(\tau) \log(x^2 + y^2) + H_i(\tau) \quad \text{as} \quad x, y \to 0, \tag{4.30}$$

for $i = 1, 2$, where F_i, H_i are related to f_i and h_i in (4.21) and (4.24), and are determined by matching (see (4.34) below). There are also initial conditions for $\tilde{W}_i$, found from matching with the solution (4.13) in time-scale 1, namely

$$\tilde{W}_1 \sim 2\pi G(x,y)\tau + O(1) \quad \text{as} \quad \tau \to +\infty, \tag{4.31}$$

$$\tilde{W}_2 \sim \pi G(x,y)(\log\tau - 1 - \log(4a(1-2a)) + 2K)\tau + O(\log\tau) \quad \text{as} \quad \tau \to +\infty, \tag{4.32}$$

where $G(x,y)$ is the Green's function defined by (4.14). Note that the limiting form (4.16) is used to derive these two conditions.

(iv) *Treatment of (initial-) boundary-value problems*

BVPs for w_a and w_b: The equations governing for w_a and w_b (4.26) are the same as those governing w_e in the previous time-scale (see (4.3)), so we have the results

$$w_a(x,y) = w_b(x,y) = w_e(x,y), \quad \tau_a = \tau_b = \hat{t}_e,$$

$$w_a = w_b \sim ax^2 + (\tfrac{1}{2} - a)y^2 \quad \text{as} \quad x, y \to 0. \tag{4.33}$$

Thus (4.25) contains the term $(\beta + 1)w_e(x,y)$ with the β corresponding to the latent heat required to freeze a unit area and the 1 to the sensible heat required to reduce the temperature from the initial value of 0 to the boundary value -1; we find by differentiating (4.25) with respect to τ that at extinction the leading order temperature is -1 in almost all of the solid.

In order to match between regions I and II we require

$$F_1(\tau) = f_1(\tau) = -\tau, \quad H_1(\tau) = h_1(\tau) + f_2(\tau), \quad F_2(\tau) = f_2(\tau). \tag{4.34}$$

With f_1 determined, we can proceed with the solution to (4.19)-(4.21), and likewise, knowledge of F_1 allows us to solve (4.28)-(4.31) for $\tilde{W}_1$.

BVP for $\bar{W}_1$: With the use of the similarity variables

$$\bar{X} = \frac{\bar{x}}{\sqrt{2\tau}}, \quad \bar{Y} = \frac{\bar{y}}{\sqrt{2\tau}}$$

the solution to (4.19)-(4.21) is simply $\bar{W}_1 = 2\tau\Psi(\bar{\phi}, \bar{\psi}; a)$, where Ψ is given by (3.7)-(3.9), $(\bar{\phi}, \bar{\psi})$ are the elliptic coordinates

$$\bar{X} + i\bar{Y} = \left(\frac{1-4a}{2a(1-2a)}\right)^{1/2} \cosh(\bar{\phi} + i\bar{\psi}), \tag{4.35}$$

and the free boundary $\tau = \Omega_0(\bar{x}, \bar{y})$ is the ellipse

$$\left(\frac{2a}{1-2a}\right)\bar{x}^2 + \left(\frac{1-2a}{2a}\right)\bar{y}^2 = 2\tau.$$

By comparing the far-field behaviour

$$\bar{W}_1 \sim a\bar{x}^2 + \left(\tfrac{1}{2} - a\right)\bar{y}^2 - \tfrac{1}{2}\tau\log(\bar{x}^2+\bar{y}^2) + \tfrac{1}{2}\tau(\log 2\tau - \log(8a(1-2a)) - 1)$$

as $\bar{x}^2+\bar{y}^2 \to \infty$ with (4.21), we can determine $h_1 = \frac{1}{2}\tau(\log\tau - \log(4a(1-2a)) - 1)$.

IBVP for $\tilde{W}_1$: The solution to (4.28)-(4.31) for $\tilde{W}_1$ is in the form

$$\tilde{W}_1 = 2\pi G(x,y)\tau + w_c(x,y), \tag{4.36}$$

where the function w_c satisfies

$$\frac{\partial^2 w_c}{\partial x^2} + \frac{\partial^2 w_c}{\partial y^2} = -2\pi G(x,y) \quad \text{in} \quad B, \quad w_c = \tau_c \quad \text{on} \quad \partial B, \tag{4.37}$$

$$w_c = \frac{\partial w_c}{\partial x} = \frac{\partial w_c}{\partial y} = 0 \quad \text{at} \quad (x,y) = (0,0). \tag{4.38}$$

Local analysis reveals that w_c will exhibit the behaviour

$$w_c \sim \tfrac{1}{4}r^2\log r - \tfrac{1}{4}(1-K)r^2 + C_0(x^2-y^2) \quad \text{as} \quad x, y \to 0. \tag{4.39}$$

Here C_0 and τ_c are constants which depend on the region B and are determined via the solution to (4.37)-(4.38). Of course in practise such a solution may be difficult to obtain; an example is presented in section 5. Examination of the behaviour of $\tilde{W}_1$ as $x, y \to 0$ reveals that $H_1 = -\tau K$, where K is defined by (4.15), which implies that

$$F_2(\tau) = f_2(\tau) = -\tfrac{1}{2}\tau(\log\tau - \log(4a(1-2a)) - 1 + 2K). \tag{4.40}$$

With f_1 and F_1 now determined, the problems for $\bar{W}_2$ and $\tilde{W}_2$ are now fully specified.

BVP for $\bar{W}_2$: The solution to (4.22)-(4.24) is

$$\begin{aligned} \bar{W}_2 &= f_2(\tau)(\bar{\phi} + \tfrac{1}{2}\log(1-4a)) \\ &= -\tfrac{1}{2}\tau(\log\tau - \log(4a(1-2a)) - 1 + 2K)(\bar{\phi} + \tfrac{1}{2}\log(1-4a)), \end{aligned}$$

with

$$\Omega_1 = f_2\left(\frac{1}{2}\left(\frac{2a}{1-2a}\bar{x}^2 + \frac{1-2a}{2a}\bar{y}^2\right)\right),$$

where $\bar{\phi}$ is the elliptic coordinate defined in (4.35), so the free boundary remains elliptic through this second time-scale, keeping the aspect ratio $(1-2a)/2a$, and the function f_2 is given by (4.40).

IBVP for $\tilde{W}_2$: The solution to (4.28)-(4.30) and (4.32) for $\tilde{W}_2$ and H_2 for all time is only possible for special cases of the geometry B (see section 5 for such an example). We can, however, extract the required information by considering these equations

in the limit $\tau \to 0$. There are two scales to consider here, namely $r = O(\tau^{1/2})$ and $r = O(1)$.

For $x, y = O(\tau^{1/2})$ with $\tau \ll 1$ we seek a solution in the form

$$\tilde{W}_2 = \tau \tilde{w}(\xi, \eta, T), \tag{4.41}$$

where ξ, η and T are the similarity variables defined by (3.1) and used in section 3, so that $\tilde{w}$ satisfies

$$\frac{\partial^2 \tilde{w}}{\partial \xi^2} + \frac{\partial^2 \tilde{w}}{\partial \eta^2} - \frac{1}{2}\xi \frac{\partial \tilde{w}}{\partial \xi} - \frac{1}{2}\eta \frac{\partial \tilde{w}}{\partial \eta} + \tilde{w} = \frac{\partial \tilde{w}}{\partial T}.$$

By writing

$$\tilde{w} \sim \tfrac{1}{2}\tilde{w}_1(\rho, \theta)T^2 + \tilde{w}_2(\rho, \theta)T + \tilde{w}_3(\rho, \theta) \quad \text{as} \quad T \to \infty \tag{4.42}$$

we arrive at the partial differential equations

$$\frac{\partial^2 \tilde{w}_i}{\partial \rho^2} + \left(\frac{1}{\rho} - \frac{1}{2}\rho\right)\frac{\partial \tilde{w}_i}{\partial \rho} + \frac{1}{\rho^2}\frac{\partial^2 \tilde{w}_i}{\partial \theta^2} + \tilde{w}_i = \tilde{w}_{i-1},$$

for $i = 1, 2, 3$, with $\tilde{w}_0$ set to zero. A combination of (4.30) and (4.40) yields the boundary conditions

$$\tilde{w}_1 \sim d_1 + O(\rho), \quad \tilde{w}_2 \sim \tfrac{1}{2}\log\rho + d_2 + O(\rho) \tag{4.43}$$

$$\tilde{w}_3 \sim \tfrac{1}{2}(\log(4a(1-2a)) + 1 - 2K)\log\rho + d_3 + O(\rho) \quad \text{as} \quad \rho \to 0, \tag{4.44}$$

where the constants d_i are to be found as part of the solution process. Note the equations for $\tilde{w}_i$ are the same as those for W_i studied in section 3c (for $i = 1, 2, 3$). The boundary conditions as $\rho \to 0$ are also of the same form, and hence application of the same reasoning provides us with the solutions

$$\tilde{w}_1 = -\tfrac{1}{16}(4-\rho^2), \quad \tilde{w}_2 = \tfrac{1}{8}(4-\rho^2)\log\rho + \tfrac{1}{16}(2-\gamma+\log 2)\rho^2 + \tfrac{1}{4}(\gamma - \log 2). \tag{4.45}$$

There is a slight difference with $\tilde{w}_3$, and the result is

$$\tilde{w}_3 = D_0(1-\tfrac{1}{4}\rho^2) + C_1\rho^2\cos 2\theta - \tfrac{1}{8}(2-\gamma-2K+\log(16a(1-2a)))(\rho^2\log\rho - 4\log\rho - 4)$$

$$+\tfrac{1}{8}\rho^2\log^2\rho - \tfrac{1}{2}\log^2\rho - \log\rho - \tfrac{1}{4}E_1(\tfrac{1}{4}\rho^2)e^{\rho^2/4} + \tfrac{1}{8}(4-\rho^2)\int_\rho^\infty \frac{E_1(\frac{1}{4}s^2)e^{s^2/4}}{s}\,ds$$

where D_0 and C_1 are constants. Here there is nothing to suggest that C_1 will vanish, as there are no higher-order problems to consider (unlike with the W_i considered in section 3c). We note that the constants d_i are given by

$$d_1 = -\tfrac{1}{4}, \quad d_2 = \tfrac{1}{4}(\gamma + 2K - \log(16a(1-2a))),$$

$$d_3 = D_0 + \tfrac{1}{16} + \tfrac{1}{8}(\gamma - 2\log 2)(2 + \gamma - 2\log 2) + \tfrac{1}{2}(2 - \gamma - 2K + \log(16a(1-2a))).$$

and that the constants D_0 and C_1 cannot be determined without knowledge of the function $\tilde{W}_2$ for all time. Comparing these values for the d_i with (4.30) and (4.40) producing the asymptotic result

$$H_2(\tau) \sim \tfrac{1}{8}\tau\log^2\tau + \tfrac{1}{4}(\gamma - 2\log 2)\tau\log\tau + O(\tau) \quad \text{as} \quad \tau \to 0,$$

the $O(\tau)$ term being dependent on the constant D_0. To match outwards we require the behaviour

$$\tilde{w}_3 \sim \tfrac{1}{8}\rho^2\log^2\rho - \tfrac{1}{8}(2-\gamma-2K+\log(16a(1-2a)))\rho^2\log\rho - \tfrac{1}{4}D_0\rho^2 + C_1(\xi^2-\eta^2) - \tfrac{1}{2}\log^2\rho$$
$$-\tfrac{1}{2}(\gamma+2K-\log(16a(1-2a)))\log\rho + D_0 + \tfrac{1}{2}(4-\gamma-2K+\log(16a(1-2a))) \quad (4.46)$$

as $\rho \to \infty$.

For $x, y = O(1)$ we have

$$\tilde{W}_2 \sim w_d(x,y) + \tau u_d(x,y) + O(\tau^2) \quad \text{as} \quad \tau \to 0 \quad (4.47)$$

with

$$\nabla^2 w_d = -u_d, \quad w_d = \tilde{W}_2(x,y,0), \quad u_d = -\frac{\partial \tilde{W}_2}{\partial \tau}(x,y,0),$$

where matching with (4.45)-(4.46) gives

$$w_d \sim \tfrac{1}{8}r^2\log^2 r - \tfrac{1}{8}(2-\gamma-2K+\log(16a(1-2a)))r^2\log r - \tfrac{1}{4}D_0 r^2 + C_1(x^2-y^2), \quad (4.48)$$

$$u_d \sim -\tfrac{1}{2}\log^2 r - \tfrac{1}{2}(\gamma+2K-\log(16a(1-2a)))\log r + D_0$$
$$+\tfrac{1}{2}(4-\gamma-2K+\log(16a(1-2a))) \quad \text{as} \quad r \to 0. \quad (4.49)$$

In summary, on the second time-scale we have had to treat initial-boundary-value problems in the outer region, in contrast to the first time-scale where the governing equations are quasi-steady. Nevertheless, the time-dependence of the inner problem in the second time-scale (region I) is found to be the same as that in the first time-scale, and so, to leading order, the evolution of the free boundary does not change; it does, however, do so on the third and final time-scale, which we now describe.

(*d*) *Time-scale 3,* $\tau = O(e^{-T_c})$

The length of this time-scale is known only once T_c has been evaluated asymptotically; see (4.52) below. It follows from (4.25), (4.33), (4.36), (4.39), (4.41)-(4.42) and (4.47)-(4.49) that we have

$$u_f \sim -1 + \frac{1}{\log(1/\epsilon)}[-\log r - K + O(r^2)]$$
$$+\frac{1}{\log^2(1/\epsilon)}[-\tfrac{1}{2}\log^2 r - \tfrac{1}{2}(\gamma+2K-\log(16a(1-2a)))\log r + O(1)] \quad (4.50)$$

$$w_f \sim \beta(ax^2+(\tfrac{1}{2}-a)y^2) + ax^2 + (\tfrac{1}{2}-a)y^2 + \frac{1}{\log(1/\epsilon)}[\tfrac{1}{4}r^2\log r - \tfrac{1}{4}(1-K)r^2 + C_0(x^2-y^2)]$$
$$+\frac{1}{\log^2(1/\epsilon)}[\tfrac{1}{8}r^2\log^2 r - \tfrac{1}{8}(2-\gamma-2K+\log(16a(1-2a)))r^2\log r - \tfrac{1}{4}D_0 r^2 + C_1(x^2-y^2)] \quad (4.51)$$

with $r = O(\epsilon)$ and $\beta \to \infty$. We reiterate that while C_0 can in principle be found by solving the elliptic boundary-value problem (4.37), the process for computing C_1 involves solving a time-dependent partial differential equation, reflecting the point

noted earlier that for general β, a_1 depends on the evolution through previous times. The logarithmic singularity in this expression for the final temperature distribution is clearly unphysical, since we know $-1 \le u_f \le 0$. This nonuniformity implies there is a further time-scale to consider, and the appropriate analysis for this is in fact that presented in section 3. By matching (4.51) with (3.24) we see that for $\beta \gg 1$ we must have

$$T_c = 2\log^2(1/\epsilon) - 2(1+\gamma-\log(16a(1-2a)))\log(1/\epsilon) + \tfrac{1}{2}(1-\tfrac{1}{6}\pi^2)\log(\log(1/\epsilon)) + O(1), \tag{4.52}$$

$$a_1 = a + \frac{1}{\beta}\left(a - \frac{1}{4}\right) + O\left(\frac{1}{\beta\log(1/\epsilon)}\right)$$

so that (4.50) and (4.51) are valid only as long as $R \ll \log^2(1/\epsilon)$. The third time-scale is therefore exponentially short, and is for

$$\tau = O(e^{-T_c})$$

(by exponentially short we mean that τ scales essentially as $e^{-2\log^2(1/\epsilon)}$). By rewriting (3.25) and (3.24) we have for $\beta \gg 1$

$$\begin{aligned} u_f &\sim -16a(1-2a)[\zeta_0(R) + \zeta_1(R)/\log(1/\epsilon) + O(\log^{-2}(1/\epsilon))]e^{-\Pi(R)} \quad (4.53)\\ w_f &\sim \beta(ax^2 + (\tfrac{1}{2}-a)y^2) + (a-\tfrac{1}{4})(x^2-y^2) \\ &\quad +4a(1-2a)r^2[\zeta_0(R) + \zeta_1(R)/\log(1/\epsilon) + O\left(\log^{-2}(1/\epsilon)\right)]e^{-\Pi(R)} \end{aligned}$$

as $r \to 0$ which are valid for all $r \ll 1$ and $\beta \gg 1$. Here the auxiliary functions ζ_0, ζ_1 and Π are defined by

$$\zeta_0(R) = \left(1 + R/\log^2(1/\epsilon)\right)^{1/2},$$

$$\zeta_1(R) = [1+\gamma-\log(16a(1-2a))][-2\zeta_0(R) + 1 + \gamma - \log(16a(1-2a))]/(4\zeta_0(R)^2) + (1-\tfrac{1}{6}\pi^2)\log\zeta_0(R) + \delta_1,$$

$$\Pi(R) = 2(\zeta_0(R)-1)\log(1/\epsilon) + [(1+\gamma)(\zeta_0(R)-1) + \log(16a(1-2a))]/\zeta_0(R),$$

where δ_1 is some constant, which can in principle be determined with the use of higher order terms in (3.19). Also, the area enclosed by the free boundary can be expressed for $\beta \gg 1$ as

$$\pi\tau\sigma^2 \sim 32a(1-2a)\pi\epsilon^2\tau[1 + S_0(T)/\log(1/\epsilon) + O(\log^{-2}(1/\epsilon))]e^{-\Pi(T/2)} \quad \text{as} \quad T \to \infty, \tag{4.54}$$

where

$$S_0(T) = (\tfrac{1}{2}(1-\tfrac{1}{6}\pi^2)\log\zeta_0(\tfrac{1}{2}T) + \delta_2)/\zeta_0(\tfrac{1}{2}T) + \tfrac{1}{4}(1+\gamma-\log(16a(1-2a)))^2/\zeta_0(\tfrac{1}{2}T)^3$$

and δ_2 is some constant (which can be determined from higher order terms in (3.20)), this expression being valid for all $\tau \ll 1$ and $\beta \gg 1$. Finally, the aspect ratio of the free boundary near extinction is

$$\frac{1-2a_1}{2a_1} = \frac{1-2a}{2a} + \frac{1}{\beta}\frac{1-4a}{8a^2} + O\left(\frac{1}{\beta\log(1/\epsilon)}\right). \tag{4.55}$$

In the radially symmetric case, the results given by (4.53) and (4.54) agree with those presented by Soward (1980).

5. Inward solidification of a rectangular domain

In this section we consider the specific example in which the initial region of fluid B is rectangular in shape, covering the domain

$$-\alpha \leq x \leq \alpha, \quad -1 \leq y \leq 1. \tag{5.1}$$

We use this example because the geometry is simple enough that the constants a, K and τ_j for $j = a, b, c, d$ can be computed explicitly. We should note, moreover, that this example is of interest in its own right, with many applications in industry (the solidification of liquid metals and freezing of foodstuffs, for example) and has been studied in detail numerically, by Wallman (1997) in particular.

An analytic solution to (4.1)-(4.2) in this case may not be available for all time; the small-time behaviour is given by problem P3 in Howison and King (1989). Separation of variables can be used to solve (4.3) to give

$$W_e = \frac{1}{2}(y^2 - 1) + \sum_{m=0}^{\infty} \frac{16(-1)^m \cos\left[\frac{1}{2}(2m+1)\pi y\right] \cosh\left[\frac{1}{2}(2m+1)\pi x\right]}{\pi^3(2m+1)^3 \cosh\left[\frac{1}{2}(2m+1)\pi\alpha\right]},$$

from which we can compute

$$\hat{t}_e = -W_e(0,0) = \frac{1}{2} - \sum_{m=0}^{\infty} \frac{16(-1)^m}{\pi^3(2m+1)^3 \cosh\left[\frac{1}{2}(2m+1)\pi\alpha\right]}.$$

The local behaviour of $w_e = W_e + \hat{t}_e$ as $x, y \to 0$ reveals that

$$a = \sum_{m=0}^{\infty} \frac{2(-1)^m}{\pi(2m+1) \cosh\left[\frac{1}{2}(2m+1)\pi\alpha\right]},$$

which reduces to $a = \frac{1}{4}$ when $\alpha = 1$, as expected (in this special case the region B is square in shape, and the free boundary just before extinction is circular).

In figure 1 we plot the aspect ratio of the free boundary near extinction for infinite Stefan number problem (4.1)-(4.2) (which is $(1-2a)/2a$) against the aspect ratio of the rectangular boundary (which is α). It is interesting to note that this relationship is strongly nonlinear with

$$\frac{1-2a}{2a} \sim \frac{\pi}{8} e^{\pi\alpha/2} \quad \text{as} \quad \alpha \to \infty. \tag{5.2}$$

The aspect ratio of the vanishing region of liquid is expected to be a decreasing function of β, being slightly more than $(1-2a)/2a$ for β large but finite, as indicated by (4.55).

Throughout section 4 we have used the constant K, defined by the solution to (4.14) for the Green's function $G(x, y)$ along with the condition (4.15). In this example we can compute G using the method of images, which gives us

$$G(x,y) = -\frac{1}{4\pi} \sum_{m=-\infty}^{\infty} \sum_{n=-\infty}^{\infty} (-1)^{n+m} \log\left[\frac{(x-2n\alpha)^2 + (y-2m)^2}{\alpha^2(2n+1)^2 + (2m+1)^2}\right],$$

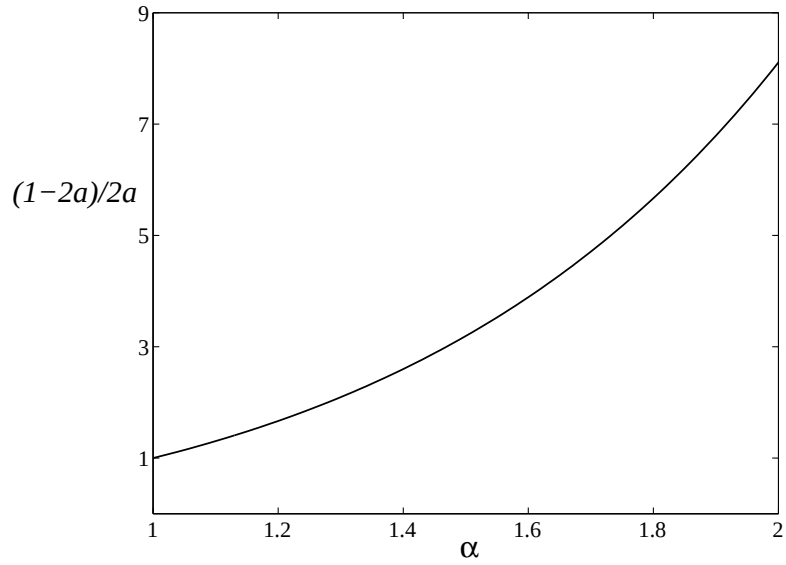

Figure 1. A plot of the aspect ratio $(1-2a)/2a$ for the free boundary just before extinction versus the aspect ratio of the domain α.

and the result that

$$K = -\log(1+\alpha^2) + \sum_{\substack{m=-\infty \\ (n,m)\neq(0,0)}}^{\infty} \sum_{n=-\infty}^{\infty} (-1)^{n+m} \log\left[\frac{4(n^2\alpha^2+m^2)}{\alpha^2(2n+1)^2+(2m+1)^2}\right].$$

We note that when $\alpha = 1$ the rectangle (5.1) becomes the unit square, and $K \approx -0.076$. To this order, the value of K is the only difference between the near extinction analysis for the square and that for the circle (a circle of radius $e^{0.076} \approx 1.079$ also has $K \approx -0.076$, and hence has the same extinction behaviour as the unit square, at least to this order).

To compute τ_c we have to solve the boundary-value problem (4.37)-(4.38). We do this with the use of the finite Fourier transform pair

$$\bar{P}(n,m) = \int_{-1}^{1}\int_{-\alpha}^{\alpha} P(x,y) \sin\left[\tfrac{1}{2\alpha}n\pi(x+\alpha)\right] \sin\left[\tfrac{1}{2}m\pi(y+1)\right]\, dxdy\,,$$

$$P(x,y) = \frac{1}{\alpha}\sum_{n=1}^{\infty}\sum_{m=1}^{\infty} \bar{P}(n,m) \sin\left[\tfrac{1}{2\alpha}n\pi(x+\alpha)\right] \sin\left[\tfrac{1}{2}m\pi(y+1)\right].$$

The result is that $w_c = W_c + \tau_c$, where

$$W_c = \frac{32}{\alpha\pi^3}\sum_{m=0}^{\infty}\sum_{n=0}^{\infty} \frac{\cos\left[\tfrac{1}{2\alpha}(2n+1)\pi x\right]\cos\left[\tfrac{1}{2}(2m+1)\pi y\right]}{((2n+1)^2/\alpha^2+(2m+1)^2)^2},$$

$$\tau_c = -\frac{32}{\alpha\pi^3}\sum_{m=0}^{\infty}\sum_{n=0}^{\infty} \frac{1}{((2n+1)^2/\alpha^2+(2m+1)^2)^2}.$$

The next order correction τ_d can also be computed with this geometry using finite Fourier transforms. The solution to (4.28)-(4.30), (4.32) when B is the rectangle (5.1) is

$$\tilde{W}_2 = \tau_d + \pi\tau(\log\tau - \log(4a(1-2a)) - 1 + 2K)G(x,y)$$

$$+\frac{\pi}{\alpha}\sum_{m=0}^{\infty}\sum_{n=0}^{\infty}\chi_{mn}(\tau)\cos\left[\tfrac{1}{2\alpha}(2n+1)\pi x\right]\cos\left[\tfrac{1}{2}(2m+1)\pi y\right],$$

where

$$\chi_{mn}(\tau) = \frac{1}{\lambda_{mn}^2}(E_1(\lambda_{mn}\tau)e^{\lambda_{mn}\tau} + \log\tau - \log(4a(1-2a)) + 2K),$$

$$\lambda_{mn} = \frac{\pi^2}{4}\left(\frac{(2n+1)^2}{\alpha^2} + (2m+1)^2\right).$$

But we know $\tilde{W}_2(x,y,0) = w_d(x,y) \to 0$ as $x, y \to 0$, so it must be that

$$\tau_d = \frac{\pi}{\alpha}\sum_{m=0}^{\infty}\sum_{n=0}^{\infty}\frac{1}{\lambda_{mn}^2}(\gamma + \log(\lambda_{mn}) + \log(4a(1-2a)) - 2K).$$

As a check on our results, we compare with calculations made by Wallman (1997). Wallman solved the extinction problem (2.1)-(2.2) numerically using an enthalpy formulation for the present case where B is the rectangle (5.1). For $\beta = 50$ and $\alpha = 2$ he found that the extinction time $t_f \approx 23.03$. Using (4.18) and the results of this section, we find to leading order $t_f \approx 22.78$, but to order $\log^{-1}(1/\epsilon)$ we find $t_f \approx 23.06$ and to order $\log^{-2}(1/\epsilon)$ $t_f \approx 23.08$. This latter calculation confirms the correction terms in (4.18) are important for moderately large values of β, and also serves as a verification of the numerical scheme used by Wallman (1997). We note that as far as we are aware there is no other data in the literature computing extinction times with large Stefan number for this example. Wallman also calculated the aspect ratio of the free boundary near extinction; the variation with β expressed in the asymptotic result (4.55) shows good agreement with these calculations.

6. Discussion

We have presented here a rather complete asymptotic analysis of the two-dimensional one-phase inward solidification problem with large Stefan number β. As shown by Soward (1980) in the radial case, the freezing process takes place on three distinct time-scales, the last of which can be described by analysis essentially independent of the Stefan number. This generic extinction analysis shows that the solid-melt interface ultimately approaches an ellipse just before complete freezing, and describes the way in which the contraction takes place. However, this analysis alone does not enable the location of the extinction point, the aspect ratio of the limiting ellipse, nor the time taken to freeze the entire body to be computed, because u_f depends on the evolution over earlier time-scales. In addition, there is a further free constant left to be determined, namely T_c, which represents a rescaling of the dimensions of the final ellipse. In the large Stefan number limit, though, we can analyse the complete freezing process (on three time-scales) and determine how

these important physical quantities depend on the initial geometry and the Stefan number. The generic extinction analysis of section 3 is, however, a vital part of the large Stefan number analysis, even though it occurs on an exponentially short time-scale. It moderates the singularity created on the second time-scale, and is necessary in order to provide a uniformly valid description of the freezing process as we near extinction.

We have found that, for large Stefan number, the aspect ratio of the elliptic free boundary near extinction is given by (4.55), where the constant a is determined through the solution of the boundary-value problem (4.3). This implies that for $\beta = \infty$ the aspect ratio is simply $(1 - 2a)/2a$, which is what we expect, as this corresponds to the result for contracting bubbles in a Hele-Shaw cell (which is described by our leading order problem in the first time-scale). As β decreases, the result (4.55) suggests that the aspect ratio near extinction increases, at least for large Stefan number. This behaviour agrees with numerical results found by Wallman (1997), who found, using a rectangular initial geometry as an example, that the aspect ratio of the free boundary near extinction increases monotonically as the Stefan number β decreases. Moreover, an asymptotic analysis of the complementary limit $\beta \to 0$, which we shall not pursue here, shows that the aspect ratio grows without bound as β decreases, the free boundary forming a slit in the limit, provided that $a \neq \frac{1}{4}$.

From (4.55) and (5.2) we see that for the case in which B is a rectangle, even a moderate amount of stretching of the initial geometry produces shrinking regions of liquid which are very long and slender (with the aspect ratio of the free boundary near extinction becoming exponentially large as the rectangle's dimension α increases). This interesting behaviour remains qualitatively the same regardless of the initial geometry B, so that freezing regions of liquid with large aspect ratios leads to small elliptic free boundaries with exponentially large aspect ratios.

Throughout our study we have assumed that the initial region B is such that the function w_e introduced in section 4b(i) has exactly one global minimum. This way the liquid region contracts continuously from B (at $t = 0$) to a single point only (at $t = t_f$). Of course in reality w_e may have more than one such minimum, in which case some sort of pinch off will occur, leading to multiple extinction points. Entov and Etingof (1991) prove the sufficient condition that if B is convex then w_e will have only one minimum, but do not provide necessary conditions. For our purposes we note only that, with the exception of special (borderline) cases, the behaviour near each extinction point should be the same as that described here.

We also note that while the leading order problem on the first time-scale is time-reversible, the full Stefan problem is not. We therefore cannot use the results of this study to infer information about the ill-posed Stefan problem in which supercooled fluid solidifies outwards. For a discussion on the ill-posed Stefan problem the reader is instead referred to the recent paper McCue *et al.* (2003).

Finally, we note that the approach presented here extends to three-dimensional domains, with some of the details simplified by the absence of logarithmic terms (the volume enclosed by the free boundary in three dimensions on the second time-scale is $O(\beta^{-3/2})$). We shall present the details of this analysis elsewhere.

The funding of the EPSRC is gratefully acknowledged. The authors would also like to thank Miguel Herrero for providing a copy of Andreucci *et al.* (2001) and Andrew Wallman for helpful conversations.

Appendix A. Determing the solution to (3.15)

Separation of variables reveals that the linearly independent homogeneous solutions W_{iH} to (3.15) with zero right-hand sides are of the form $R_n(\rho)(A_{in}\cos n\theta + B_{in}\sin n\theta)$, where $R_n(\rho)$ satisfies

$$\frac{d^2R_n}{d\rho^2} + \left(\frac{1}{\rho} - \frac{1}{2}\rho\right)\frac{dR_n}{d\rho} + \left(1 - \frac{n^2}{\rho^2}\right)R_n = 0 \tag{A 1}$$

and n is a non-negative integer. Linearly independent solutions to this ordinary differential equation with no exponential growth are

$$R_0 = 1 - \frac{1}{4}\rho^2, \quad R_2 = \rho^2$$

for $n = 0$ and $n = 2$ and

$$R_n = e^{\rho^2/8}W_{\frac{3}{2},\frac{1}{2}n}(\tfrac{1}{4}\rho^2)/\rho$$

for all other values of n, where $W_{k,\mu}(z)$ is Whittaker's function (see Abramowitz and Stegun 1970). These latter solutions have the algebraic singularities

$$R_n \sim \frac{2^{n-1}\Gamma(n)}{\Gamma(\frac{1}{2}n-1)}\frac{1}{\rho^n} \quad \text{as} \quad \rho \to 0,$$

where $\Gamma(z)$ denotes the usual Gamma-function (again, see Abramowitz and Stegun 1970).

The solution for W_1 which satisfies the conditions as $\rho \to 0$ is

$$W_1 = 1 - \tfrac{1}{4}\rho^2 + (A_{12}\cos 2\theta + B_{12}\sin 2\theta)\rho^2,$$

the constants $A_{1n}, B_{1n} = 0$ for $n = 1$ and $n \geq 3$, since algebraic singularities as $\rho \to 0$ are unacceptable.

A particular solution for W_2, denoted by W_{2P}, is then given by

$$\begin{aligned} W_{2P} &= \tfrac{1}{2}\rho^2\log\rho - 2\log\rho - 2 + (A_{12}\cos 2\theta + B_{12}\sin 2\theta)\left(\frac{16}{\rho^2} + 8 - 2\rho^2\log\rho\right) \\ &\sim 16(A_{12}\cos 2\theta + B_{12}\sin 2\theta)\frac{1}{\rho^2} - 2\log\rho + O(1) \quad \text{as} \quad \rho \to 0. \end{aligned} \tag{A 2}$$

We see now that no choice of A_{2n} and B_{2n} in W_{2H} makes the $O(\rho^{-2})$ terms in (A 2) vanish, as required by the boundary conditions (3.13)-(3.14), because the A_{2n} and B_{2n} are simply constants which cannot cancel the θ-dependent terms. We must therefore set $A_{12} = B_{12} = 0$, so that W_1 is radially symmetric, as indicated by (3.16). A similar argument holds for the solution to W_3 and any higher-order terms, with the radial symmetry of W_i following as a solvability condition on W_{i+1}, for $i \geq 1$. However, we do not present the details here.

References

Abramowitz, M. and Stegun, I. 1970 *Handbook of mathematical functions*. Dover.

Allen, D. N. de G. and Severn, R. T. 1962 The application of relaxation methods to the solution of non-elliptic partial differential equations-III. *Q. Jl Mech. Appl. Math.* **15**, 53-62.

Andreucci, D., Herrero, M. A. and Velázquez, J. J. L. 2001 The classical one-phase Stefan problem: a catalog of interface behaviors. *Surv. Math. Ind.* **9**, 247-337.

Carslaw, H. S. and Jaeger, J. C. 1973 *Conduction of heat in solids.* Oxford University Press.

Crank, J and Gupta, S. 1975 Isotherm migration method in two dimensions. *Int. Jl Heat Mass Trans.* **18**, 1101-1107.

Crowley, A. B. 1978 Numerical solution of Stefan problems. *Int. Jl Heat Mass Trans.* **21**, 215-219.

Davis, G. B., and Hill, J. M. 1982 A moving boundary problem for the sphere. *IMA Jl Appl. Math.* **29**, 99-111.

Entov, V. M. and Etingof, P. I. 1991 Bubble contraction in Hele-shaw cells. *Q. Jl Mech. Appl. Math.* **44**, 507-535.

Herrero, M. A. and Velázquez, J. J. L. 1997 On the melting of ice balls. *SIAM J. Math. Anal.* **28**, 1-32.

Hill, J. M., and Dewynne, J. N. 1986 On the inward solidification of cylinders. *Q. Appl. Math.* **44**, 59-70.

Hoang, H. V., Hill, J. M. and Dewynne, J. N. 1998 Pseudo-steady-state solutions for solidification in a wedge. *IMA Jl Appl. Math.* **60**, 109-121.

Howison, S. D. and King, J. R. 1989 Explicit solutions to six free-boundary problems in fluid flow and diffusion. *IMA Jl Appl. Math.* **42**, 155-175.

King, J. R., Riley, D. S. and Wallman, A. M. 1999 Two-dimensional solidification in a corner. *Proc. R. Soc. Lond.* A **455**, 3449-3470.

Lazaridis, A. 1970 A numerical solution of the multidimensional solidification (or melting) problem. *Int. Jl Heat Mass Trans.* **13**, 1459-1477.

McCue, S. W., King, J. R. and Riley, D. S. 2003 Extinction behaviour of contracting bubbles in porous media. *Q. Jl Mech. Appl. Math.* **56**, 455482

Pedroso, R. I. and Domoto, G. A. 1973 Perturbation solutions for spherical solidification of saturated liquids. *J. Heat Trans.* **95**, 42-46.

Riley, D. S. and Duck, P. W. 1976 Application of the heat-balance integral method to the freezing of a cuboid. *Int. J. Heat Mass Trans.* **20**, 294-296.

Riley, D. S., Smith, F. T. and Poots, G. 1974 The inward solidification of spheres and circular cylinders. *Int. Jl Heat Mass Trans.* **17**, 1507-1516.

Soward, A. M. 1980 A unified approach to Stefan's problem for spheres. *Proc. R. Soc. Lond.* A **373**, 131-147.

Stewartson, K. and Waechter, R. T. 1976 On Stefan's problem for spheres. *Proc. R. Soc. Lond.* A **348**, 415-426.

Wallman, A. M. 1997 Moving boundary problems in heat transfer and fluid flow. PhD thesis, University of Bristol.

Wallman, A. M., King, J. R. and Riley, D. S. 1997 Asymptotic and numerical solutions for the two-dimensional solidification of a liquid half-space. *Proc. R. Soc. Lond.* A **453**, 1397-1410.